Ingrid Stober
Kurt Bucher

Geothermal Energy

From Theoretical Models to Exploration and Development

Second Edition

Springer

Geothermal Energy

Ingrid Stober · Kurt Bucher

Geothermal Energy

From Theoretical Models to Exploration and Development

Second Edition

Springer

Ingrid Stober
Institute of Geo- and Environmental Sciences, University of Freiburg
Freiburg, Baden-Württemberg, Germany

Kurt Bucher
Institute of Geo- and Environmental Sciences, University of Freiburg
Freiburg, Baden-Württemberg, Germany

ISBN 978-3-030-71684-4 ISBN 978-3-030-71685-1 (eBook)
https://doi.org/10.1007/978-3-030-71685-1

Cover illustration: Steam clouds from two wells of the Krafla geothermal power plant (N-Iceland)

This Springer imprint is published by the registered company Springer Nature Switzerland AG
The registered company address is: Gewerbestrasse 11, 6330 Cham, Switzerland

Preface

Geothermal energy is an inexhaustible source of thermal and electrical energy on a human time scale. Its utilization is friendly to the environment and supplies base-load energy. The energy source does not depend on weather, and the energy is supplied 24 hours per day during 7 days a week. Utilization of geothermal energy increases the regional and local net product. It relieves dependence from fossil fuels and helps to conserve the valuable fossil chemical resources. Deep geothermal resources provide thermal and electrical (converted thermal) energy, thus providing reliable and sustainable energy for the future.

Electrical energy from geothermal resources provides an important contribution to the base-load electrical energy supply and replaces large-scale power plants fired with fossil fuels. A particularly prominent ranking regarding the production of electrical energy holds the global high-enthalpy regions associated with active volcanism in dynamic tectonic areas. However, geothermal energy can be utilized worldwide and produced at various depths with different specific technical systems. Geothermal systems may be used for covering the heat demand of single buildings or entire districts. Solitary systems can be combined with large groups of systems, e.g., geothermal probes can be arranged to larger probe fields making it possible to heat and cool larger building complexes depending on actual needs.

Utilization of deep geothermal resources extracts hot fluid from thermal reservoirs. These hot waters are re-injected to the reservoirs, thus maintaining the natural balance and permitting a sustainable and economical management of the resource. Heat and electricity from geothermal sources have the potential to cover a substantial share of the worldwide base-load energy demand also outside the high-enthalpy regions. Fossil-fuel-fired power plants may be used covering peak period requirements only.

The utilization of geothermal energy from shallow resources for the production of energy at low temperature for heating and cooling applications made tremendous progress in the past decades.

Geothermal energy from deep sources and reservoirs can contribute significant base-load energy. The necessary technology of Enhanced Geothermal Systems (EGS) can be installed nearly everywhere. However, EGS technology needs further improvements and research. Successful demonstration projects would help to popularize EGS further.

Long-term concepts of energy politics integrate geothermal energy sources because it supplies base-load energy. Intelligent combination of geothermal systems with other sources of renewable energy can create diverse sustainable synergy benefits. For residential homes, for example, combining ground-source heat pump systems with solar-thermal systems proved to be highly energy efficient. Geothermal power from a deep hydrothermal system can be combined with a biogas installation improving the energy efficiency. The deep fluid reservoir can be used as a rechargeable aquifer storage facility for extracting heat in the cold season and recharging it in the warm season. Such combined systems strike out in a new direction ranging from heat management for single houses to large-scale city planning.

This book aims to offer the reader a general overview over the many different aspects of utilization of geothermal energy. We are looking forward to the further rapid development of this fascinating source of energy in the years to come. We wish all of us a reliable, safe and environmentally friendly supply of thermal and electrical power. We hope to contribute to the sustainable use of energy with this book.

Freiburg, Germany

Ingrid Stober
Kurt Bucher

Contents

Chapter 1
Thermal Structure of the Earth

Island of Vulcano, southern Italy

I. Stober and K. Bucher, *Geothermal Energy*,
https://doi.org/10.1007/978-3-030-71685-1_1

1.1 Renewable Energies, Global Aspects

The term "renewable energy" is used for a source of energy from a reservoir that can be restored on a "short time scale" (in human time scales). Renewable energy includes geothermal energy and several forms of solar energy such as bio-energy (bio-fuel), hydroelectric, wind-energy, photovoltaic and solar-thermal energy. These sources of energy are converted to heat or electricity for utilization. An example: The "renewable" aspect of burning firewood in a cooking stove lies in the relatively short period of time required to re-grow chopped down forests with solar energy and the process of photosynthesis. In contrast, it will take much more time to "renew" coal beds when burning coal for the same purpose, although geological processes will eventually form new coal beds. The "renewable" aspect of geothermal energy will be explained and discussed in detail in this chapter.

The International Geothermal Association (IGA) wrote in the Status Report Ren21 (2017) on "Renewable Energy Policy Network for the 21st Century" that the global production of renewable energy increased by 168 GW_{el} (+9.1%) from 2015 to 2016. The total worldwide production of electricity from renewable resources in 2019 was 7028 TWh (1 Wh = 3600 J), corresponding to 26% of the global power production capacity. China registered the highest growth rate in the production of electricity from renewable resources (BP, Statistical Review of World Energy 2020). The growth in renewable energy consumption is larger than the increase in fossil fuel consumption in Europe and the US. Political and financial programs support the development and use of energy production from renewable resources in more than 60 countries.

Hydroelectric systems had the largest share in installed capacity for electricity power production from renewable energy sources in 2016 with 1098 GW_{el} followed by wind energy with 487 GW_{el}, photovoltaic systems (303 GW_{el}) and biomass conversion with 112 GW_{el}. Geothermal systems (13.5 GW_{el}) follow with a large gap, however, also increased by 35% from 2008. Thermal energy production from renewable sources is dominated by biomass (90%), followed by solar thermal systems (2%) and geothermal systems (2%) (Ren21 2017; U.S. Department of Energy 2016).

Geothermal energy has the potential to become a significant source of energy in the future because it is available everywhere and withdrawals are continuously replenished. From a human perspective the resource is essentially unlimited. Heat and electricity can be continuously produced and therefore it is a base load resource. The utilization is friendly to the environment and the land consumption for the surface installations is small. The coming years will show how the optimistic expectations and the positive perception of geothermal energy utilization will succeed in regions with low-enthalpy geothermal resources.

1.2 Internal Structure of the Earth

Geothermal energy is the thermal energy stored in the Earth body, geothermal energy is underground heat. 99% of the Earth is hotter than 1000 ℃ and only 0.1% is colder than 100 ℃. The average temperature at the Earth surface is 14 ℃. The surface temperature of the sun is about 5800 ℃, which corresponds to the temperature at the center of the Earth (Fig. 1.1).

The Earth has a layered internal structure (Fig. 1.1) with a solid core of high-density material, an iron-nickel alloy surrounded by an outer core of the same material in a low-viscosity state. A thick internally layered, viscous magnesium silicate mantle encloses the core. The surface zone of the planet is build up of a thin rigid crust, whose composition is different on continents and oceans. This layered structure developed from a more homogeneous system by gravitational compaction and differentiation during the earliest history of the planet.

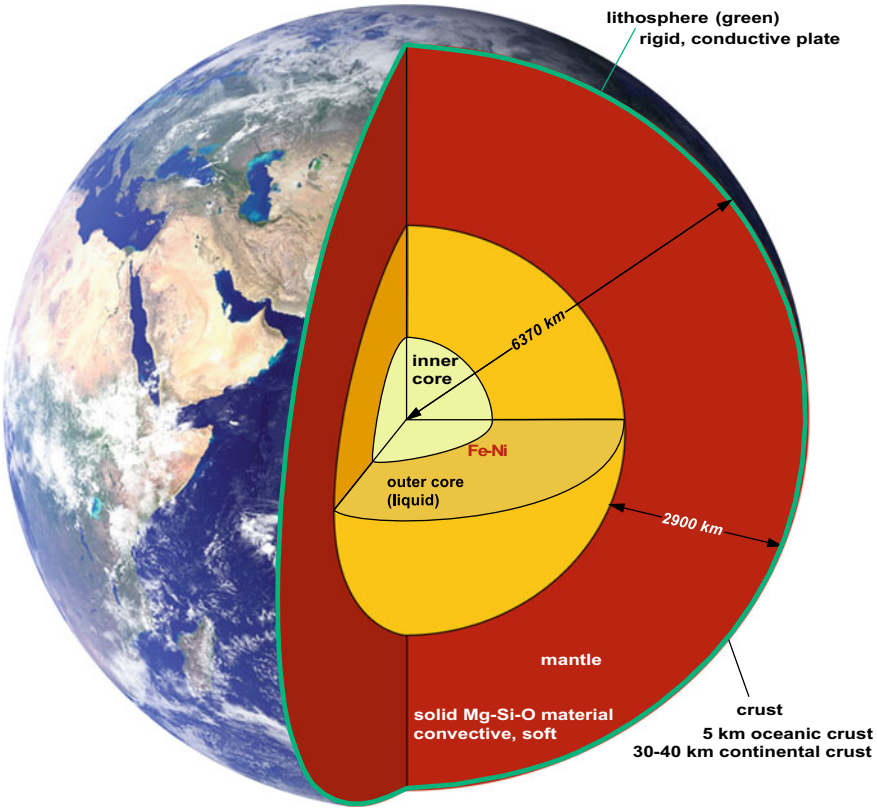

Fig. 1.1 Internal structure of the Earth

The total thickness of the core (Fig. 1.1) exceeds the thickness of the mantle. However, the core represents only about 16% of the volume of the Earth and, because of its high density about 32% of the mass of the planet.

At 6000 km depth the inner core temperatures are above 5000 ºC and the pressure is about 400 GPa. Iron meteorites that arrive at the Earth surface occasionally from space consist of material similar to the Ni–Fe alloy of the core (Fig. 1.2). The molten Fe–Ni metal outer core (about 2900 ºC) is together with the rotational movement of the planet responsible for the Earth's magnetic field. The core–mantle boundary is a zone of dramatic changes in composition and density where molten metal from the outer core and solid mantle silicate minerals mix. Beneath the lithosphere, the upper mantle reaches to a depth of about 1000 km. The boundary layer between lithospheric and convective mantle at 100–150 km depth is rheologically soft and melt may be present locally facilitating movement of the lithospheric plates. The solid but soft mantle is in a very slow convective motion driven by the heat of the core and transmitted through the core–mantle boundary (hot plate). A part of the heat given off to the mantle arises from the enthalpy of crystallization at the boundary between inner solid and outer liquid core in an overall environment setting of a cooling planet. The motor for mantle convection operates since the formation of the Earth.

The lithosphere is the rigid lid of the planet that is subdivided into a series of mobile plates that move individually as a result of pull and drag forces exerted by the convecting mantle (Fig. 1.3). The lithospheric mantle is separated from the crust by the petrographic MOHO and consists of the same rock types as the mantle as a

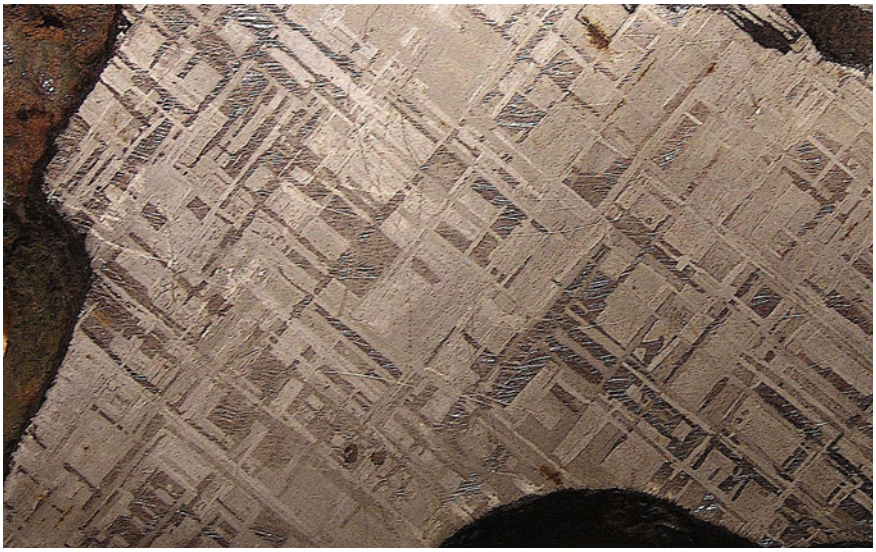

Fig. 1.2 Widmanstätten pattern made visible on an iron meteorite. The texture results from the intergrowth of the two minerals kamacite and taenite with different Fe/Ni ratios. Picture about 5 cm across

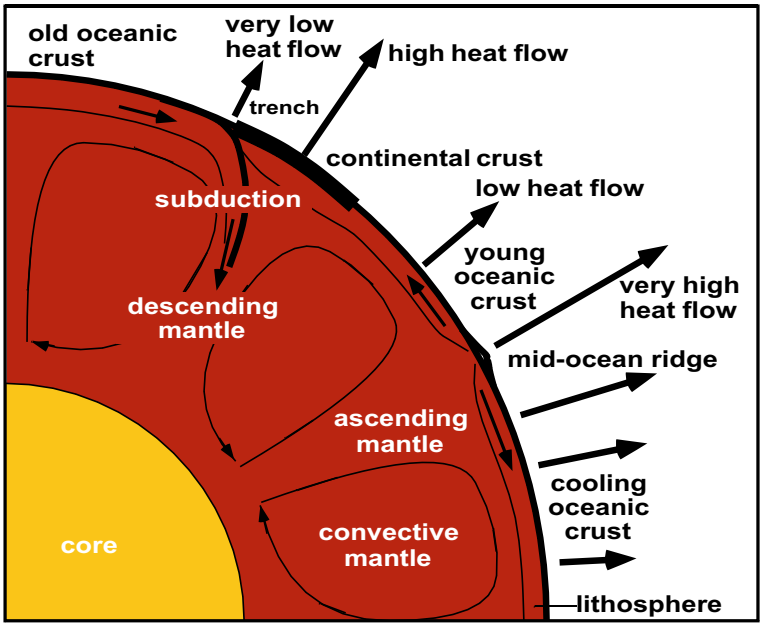

Fig. 1.3 Convection currents in the viscous mantle drive plate tectonics (movement of rigid lithospheric plates, the outermost shell of the planet) and controls large-scale heat flow (black arrows)

whole. The convecting mantle creates distinct thermal regimes at the Earth surface resulting from upwelling and subsiding hot mantel material and from the mechanical and thermal response of the lithosphere.

Convergent plate motions may create mountain belts such as the Alps and the Himalayas. The dense oceanic lithosphere of two convergent plates may be subducted and recycled into the mantle. Melting and release of H_2O from the subducting slab can generate massive amounts of melts in the overriding plate and the transfer of heat to shallow levels of the crust. Examples are the volcanic chain of the Cascades, parts of the Andes, Aleutian Islands, Japan, Philippines, Indonesia, North Island of New Zealand and many other volcanic areas of the world. Extending lithosphere creates rift and graben structures typically with a pronounced thermal response at the surface. Examples of this setting include the East African rift valley and the Basin and Range Province in the western USA.

Extensional oceanic plate margins are mid-ocean ridges and the sites of the most prominent volcanic activity on the planet. The Mid-Atlantic Ridge and the East Pacific Rise are examples of these settings (Fig. 1.4). Particularly spectacular large scale geologic structures are tied to focused upwelling systems of hot mantle, so called mantle diapirs or "hot spots". A hot spot under oceanic lithosphere is causing intraplate volcanism on the Hawaii islands, a hot spot under continental lithosphere is causing extremely dangerous rhyolite volcanism in the Yellowstone area (USA) with all associated forms of hydrothermal activity such as geysers (Fig. 1.5), mud volca-

Fig. 1.4 Basaltic lava eruption from the Earth mantle at the mid-Atlantic ridge on Iceland (Krafla eruption 1984). Lava production follows an extensional fissure

Fig. 1.5 Different stages of an eruption of Echinus Geyser in the Norris Geyser Basin, Yellowstone National park, Wyoming, USA

noes, gas vents and others. The massive Yellowstone eruptions, that have devastated the whole Earth, have a periodicity of about 600 Ka. The last one occurred about 0.6 Ma ago. The crown of the hot spots is located underneath Iceland where it coincides with the extension of the mid Atlantic ridge causing an abnormally high volcanic activity and a massive heat transfer to very shallow levels of the crust. The ash cloud of the eruption of Eyjafjallajökull stopped all air traffic in Europe in 2010. The Italian volcanoes are classic examples of volcanism and associated hydrothermal and degassing phenomena (Fig. 1.6).

1.3 Energy Budget of the Planet

The average temperature at the Earth surface is 14 ˚C, at the core–mantle boundary the temperature is in the range of 3000 ˚C. This temperature difference between the surface and the interior is the driving force for heat flow, which tries to eliminate ΔT. The process is known as so-called Fourier conduction. Heat is continuously transported from the hot interior to the surface. The terrestrial heat flow is the amount of energy (J) transferred through a unit surface area of 1 m^2 per unit time (s) and is referred to as heat flow density (q). In its general form, the Fourier equation is:

$$q = -\lambda \nabla T \quad \left(Js^{-1}m^{-2}\right) \tag{1.1a}$$

where λ is a material constant explained below. The general form can be rewritten for the case of one-dimensional flow and along a constant temperature gradient as:

$$q = -\lambda \Delta T/\Delta z \quad \left(Js^{-1}m^{-2}\right) \tag{1.1b}$$

where $\Delta T/\Delta z$ is a constant temperature gradient in vertical (z) direction.

The average global surface heat flow density is about 65 10^{-3} W m^{-2} (65 mW m^{-2}). The planet looses heat because of this heat transfer from the interior to the surface. On the other hand, the planet gains some energy by capturing solar radiation. Electromagnetic solar radiation is created in the sun by nuclear fusion reactions that are ultimately converted to other forms of energy on the planet Earth such as coal, oil, gas, wind, hydroelectric, biomass (crop, wood), photovoltaic and solar thermal. The average global solar energy received by the Earth is 170 W m^{-2}, 2600 times the amount lost by heat flow from the interior. This corresponds to 5.4 GJ per year per 1 m^2 surface area, which is approximately the energy that can be extracted from one barrel of oil, 200 kg of coal, or 140 m^3 of natural gas (source: World Energy Council). The total integrated heat flow of the planet corresponds to the impressive thermal power of 40 terra Watt (4 10^{13} W).

The measured surface heat flow density has several contributions. Only a small part of it is related to the Fourier heat flow from core and mantle as described above (about 30%). 70% is caused by heat generated by the decay of radioactive elements in the crust, mostly in the continental “granitic” crust. Specifically uranium (^{238}U,

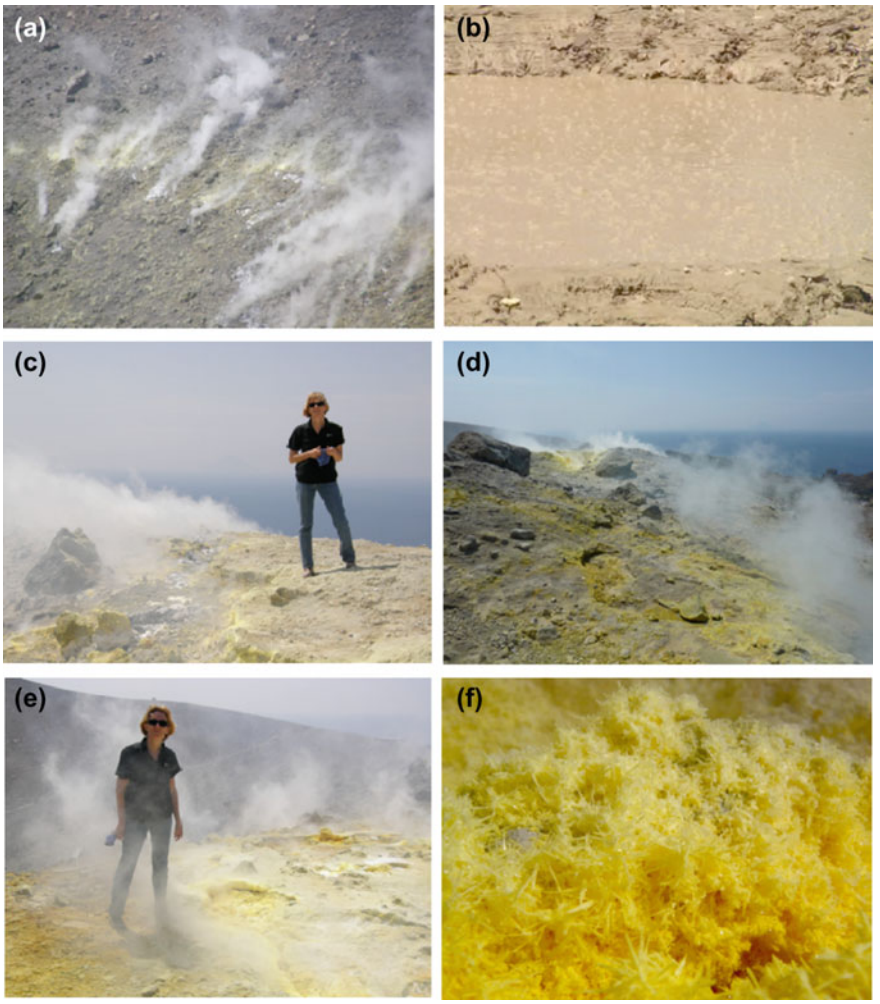

Fig. 1.6 Volcanic phenomena on the island of Vulcano (Italy): **a** Volcanic steam degassing from crater flank, **b** volcanic gasses bubble from hot water pond, **c** Steam degassing on the crater ridge, **d** Sulfur crusts on the crater ridge, **e** One of the authors submerged in poisonous volcanic gasses (photograph taken by the other author), **f** Sulfur crystals deposited from the oxidation of primary H_2S gas with atmospheric oxygen ($2H_2S + O_2 = S_2 + 2H_2O$)

^{235}U), thorium (^{232}Th) and potassium (^{40}K) in the continental crust produce ~900 EJ a^{-1} (9×10^{20} J a^{-1}). Together with the contribution of the interior of ~3×10^{20} J a^{-1}, the planet looses 1.2×10^{21} J a^{-1} (1.2 ZJ a^{-1}) thermal energy to the space. Most of it is restored in the crust continuously.

Heat production in the crust is thermal energy produced per time and volume (J s^{-1} m^{-3}). The crust is composed very differently and its thickness differs considerably. Continental crust is typically thick, granitic and rich in radioactive elements, oceanic

crust is thin, basaltic and poor in radioactive elements (Mareschal & Jaupart 2013). Therefore heat production of crustal rocks differs over a wide range (Table 1.2). The total global radioactive heat production is estimated to be on the order of 27.5 TW (Ahrens 1995).

Surface heat flow q (W m^{-2}) composed of the heat flow from the interior and the heat production in the crust varies within a surprisingly narrow range of 40–120 mW m^{-2}. This is a factor of 3 only. The global average of 65 mW m^{-2} corresponds to an average temperature increase in the upper part of the Earth crust of about 3 °C per 100 m depth increase. Departures from this average value are designated to heat flow anomalies or thermal anomalies. The variation is caused by the different large-scale geological settings as outlined above and by the diverse composition of the crust. Negative anomalies, colder than average, are related to old continental shields, deep sedimentary basins and oceanic crust away from the spreading ridges. Positive anomalies, that are hotter than the normal geotherm, are the prime targets and the major interest of geothermal exploration. Extreme heat flow anomalies are related to volcanic fields and to mid ocean ridges. In low-enthalpy areas heat flow anomalies are often related to upwelling fluids (upwelling groundwater). The adjective fluid flow also transports thermal energy to near surface environments.

Average heat flow density is 65 mW m^{-2} at the surface of continents (see above) and 101 mW m^{-2} from oceanic crust. The global average of 87 mW m^{-2} corresponds to a global heat loss of 44.2×10^{12} W (Pollack et al. 1993). A net heat loss of 1.4×10^{12} W (Clauser 2009) of the planet results from the difference between the heat lost to space and the heat production due to radioactive decay and other internal sources. The cooling process of the planet is very slow however. During the last 3 Ga (from a total of 4.6 Ga) the average mantle cooled 300–350 ˚C. The heat loss by thermal radiation from the interior is minimal (by a factor of 4000) compared with the thermal energy gained by solar radiation.

The total amount of heat (thermal energy) stored by the planet is about 12.6×10^{24} MJ (Armstead 1983). Therefore, the geothermal energy resources of the planet are truly enormous and omnipresent. Geothermal energy is everywhere available and can be extracted at any spot of the planet. Geothermal energy is friendly to the environment and it is available 24 h a day 365 days per year anywhere on the planet. Today it is used insufficiently but geothermal energy has a hot future.

1.4 Heat Transport and Thermal Parameters

A prerequisite for the design of geothermal installations is availability of data and information on the physical properties of rocks. Rock properties are required at sites of shallow geothermal installations and deep geothermal systems for heat and electricity production alike. Particularly needed are rock properties that relate to transport and storage of heat and fluids in the subsurface. Thermal properties include thermal conductivity, heat capacity and heat production; hydraulic properties embrace for

example porosity and permeability. Important properties of deep fluids are their density, viscosity and compressibility.

Geothermal heat can be transported by two basic mechanisms: (1) by heat conduction through the rocks and (2) by a moving fluid (groundwater, gasses), a mechanism referred to as advection. Conductive heat flow can be described by the empirical transport equation: $q = -\lambda \Delta T$ (Fourier law). It expresses that the heat flux (Watt per unit area of cross section) is caused by a temperature gradient ΔT between different parts of a geologic system and that it is proportional to a material property λ called thermal conductivity [J s^{-1} m^{-1} K^{-1}]. Thermal conductivity λ depicts the ability of rocks to transport heat. It varies considerably between different types of rock (Table 1.1). Rocks of the crystalline basement such as granites and gneisses conduct heat 2–3 times better than unconsolidated material (gravel, sand). Measured thermal conductivities for the same rock type may vary over wide ranges (Table 1.1) because of variations in the modal composition of rocks, different degrees of compaction, cementation or alteration, but also because of anisotropy caused by layering and other structures of the rocks. The thermal conductivity of stratified, layered or foliated rocks depends on its direction. It is generally anisotropic. In schists, for instance λ vertical to the schistosity can be only a third or less than λ parallel to the schistosity. Thick schist formations hamper vertical heat flux from the interior to the surface and thus have an insulating effect. The positive thermal anomaly at Bad Urach (SW

Table 1.1 Thermal conductivity and heat capacity of various materials

Rocks/fluids	Thermal conductivity λ (J s^{-1} m^{-1} K^{-1})	Specific heat capacity (kJ kg^{-1} K^{-1})
Gravel, sand dry	0.3–0.8	0.50–0.59
Gravel, sand wet	1.7–5.0	0.85–1.90
Clay, loam moist	0.9–2.3	0.80–2.30
Limestone	2.5–4.0	0.80–1.00
Dolomite	1.6–5.5	0.92–1.06
Marble	1.6–4.0	0.86–0.92
Sandstone	1.3–5.1	0.82–1.00
Shale	0.6–4.0	0.82–1.18
Granite	2.1–4.1	0.75–1.22
Gneiss	1.9–4.0	0.75–0.90
Basalt	1.3–2.3	0.72–1.00
Quartzite	3.6–6.6	0.78–0.92
Rocksalt	5.4	0.84
Air	0.02	1.0054
Water	0.59	4.12

Data for 25 °C 1 bar. *Source* VDI4640 2001, Schön 2004, Kappelmeyer & Haenel 1974, Landolt-Börnstein 1992

Table 1.2 Typical radiogenic heat production of selected rocks

Rock type	Heat Production ($\mu J\ s^{-1}\ m^{-3}$)
Granite	3.0 (< 1–7)
Gabbro	0.46
Granodiorite	1.5 (0.8–2.1)
Diorite	1.1
Gneiss	4.0 (< 1–7)
Amphibolite	0.5 (0.1–1.5)
Serpentinite	0.01
Sandstone	1.5 (0.2–2.3)
Shale	1.8

Source Kappelmeyer & Haenel 1974; Rybach 1976

Germany), for example, has been associated with the presence of thick shale series in the section (Schädel & Stober 1984).

All rocks contain a certain amount of voids in the form of pores and fractures. It is crucial for the heat transport properties of the rocks if the voids are filled with a liquid fluid (water) or gas (air). Air is an isolator with a very low λ value (Table 1.1). This is why in shallow geothermal systems the position and variation of the water table has a profound effect on the thermal conductance of unconsolidated rocks.

Thermal conductivity λ of air is 100 times smaller and the one of water is 2–5 smaller than that of rocks (Table 1.1). As a result the thermal conductivity of dry, air filled gravel and sand is about 0.4 $J\ s^{-1}\ m^{-1}\ K^{-1}$, however, for wet, water saturated gravel the thermal conductivity may be 2.1 $s^{-1}\ m^{-1}\ K^{-1}$ or higher. Knowing the water table and its temporal variation is critically important for determining the heat extraction capacity of a geothermal probe (subsection 6.3.2). This is extremely so in strongly karstified rocks.

The thermal conductivity (k) controls the supply of thermal energy for a given temperature gradient. The heat capacity (C) is a rock parameter that portrays the amount of heat that can be stored in the subsurface. It is the amount of heat ΔQ (thermal energy J) that is taken up or given off by a rock upon a temperature change ΔT of one Kelvin:

$$C = \Delta Q/\Delta T \quad \left(JK^{-1}\right) \tag{1.2a}$$

The specific heat capacity (c) also simply specific heat of rocks (material) is the heat capacity per unit mass. It characterizes the amount of heat ΔQ that is taken up per mass (m) of rock per temperature increase ΔT:

$$c = \Delta Q/(m\Delta T) \quad \left(Jkg^{-1}K^{-1}\right) \tag{1.2b}$$

If C is normalized to a constant volume (V) rather then mass, it is designated volumetric heat capacity also volume-specific heat capacity (s):

$$s = \Delta Q/(V\Delta T) \quad \left(Jm^{-3}K^{-1}\right) \tag{1.2c}$$

The two parameters are connected by the equation ($c = s/\rho$), where ρ is the density (kg m^{-3}). Heat capacity and thermal conductivity depend on pressure and temperature. Both parameters decrease with increasing depth in the crust. As a consequence, for a specific material the temperature rises as depth decreases.

Table 1.1 lists specific heat capacities of common rocks. For solid rocks c typically varies between 0.75 and 1.00 kJ kg^{-1} K^{-1}. The heat capacity of water c = 4.19 kJ kg^{-1} K^{-1} is 4–6 times higher than c of solid rocks. Water stores many times more heat than rocks. Referred to the volumetric heat capacity water stores about twice the amount of heat than rocks. Consequently, highly porous aquifers of unconsolidated rock store more thermal energy than low-porosity aquifers with poor hydraulic conductivity consisting of dense rocks.

Heat flow density (q) and thermal conductivity (λ) reflect the temperature distribution at depth. The temperature gradient is the temperature increase per depth increment (grad T or ΔT) at a specified depth. Equation 1.3 shows that T at a specific given depth (for constant one dimensional gradients) is given by the heat flow density and the thermal conductivity:

$$\Delta T/\Delta z = q/\lambda \quad \left(Km^{-1}\right) \tag{1.3}$$

For example: With the average continental surface q = 0.065 (W m^{-2}), λ = 2.2 (J s^{-1} m^{-1} K^{-1}) for typical granite and gneiss (Table 1.1) a constant $\Delta T/\Delta z = 0.03$ (K m^{-1}) or 3 °C per 100 m depth increase follows from Eq. 1.3. The temperature increases in the upper kilometers of the central European continental crust with 2.8–3.0 °C per 100 m of Δz, consistent with the typical mean λ-values of crustal hard rock material (Table 1.1) and the typical measured surface heat flow density of 65 mW m^{-2}. Vice versa, Eq. 1.1b or 1.3 can be used to roughly calculate q for given T-gradients and rock material.

Temperature gradients, heat flow density and hence the temperature distribution in the subsurface is not uniform. If the deviation from average values is significant the features are termed positive or negative temperature (thermal) anomaly. There are numerous geologic causes of positive thermal anomalies including active volcanism (as described above) and upwelling hot deep waters in hydrothermal systems. Upwelling thermal waters are typically related to deep permeable fault structures often in connection with graben or basin structures or boundary fault systems of mountain chains. Hydrothermal waters commonly reach the surface and discharge as hot springs. Positive anomalies can also be caused by the presence of large volumes of rock with a high thermal conductivity such as rock salt deposits. Salt diapirs preferentially conduct more heat to the surface than other surrounding sedimentary rocks. So that high heat flow is channelized in the salt diapirs. Thick insulating strata in sedimentary sequences such as shales with low thermal conductivity (often strongly anisotropic as discussed above) may retard heat transfer to the surface. Unusually high local geochemical or biogeochemical heat production can also be a reason of heat anomalies. Positive anomalies are prime target areas

for geothermal projects because their exploration and development require smaller drilling depth (Chap. 5).

All rocks contain a certain measurable amount of radioactive elements. The energy liberated by the decay of unstable nuclei is given off as ionizing radiation and then absorbed and transformed to heat. In common rocks the heat production of the decay chains of the nuclei ^{238}U, ^{235}U and ^{232}Th and the isotope ^{40}K in potassium are the only significant contributions. Uranium and thorium occur in accessory minerals, mainly zircon and monazite, in common rocks such as granite and gneiss. Potassium is a major element in common rock forming minerals including K-feldspar and mica.

Total radioactive heat production of a rock can be estimated from the concentrations of uranium c_U (ppm), thorium c_{Th} (ppm) and potassium c_K (wt.%) (Landolt-Börnstein 1992):

$$A = 10^{-5}\rho(9.52\,c_U + 2.56\,c_{Th} + 3.48\,c_K) \quad \left(\mu J s^{-1} m^{-3}\right) \tag{1.4}$$

where ρ is the density of the rock (kg m^{-3}). Some typical values for radiogenic heat production of selected representative rocks are listed in Table 1.2.

Because radiogenic heat production is related to the amount of K-bearing minerals and zircon in a rock, granite and other felsic rocks, they produce more heat than gabbros and mafic rocks (Sect. 1.3). Mantle peridotite and its hydration product serpentinite produce less than 0.01 μW m^{-3} (Table 1.2). A part of the radioactive elements can be mobilized by water–rock interaction and dissolve in hydrothermal fluids. Some thermal waters contain a considerable amount of radioactive components and are thus radioactive (Sect. 10.2).

The heat transport equation describes the variation of temperature in a rock in space and time (Carslaw & Jaeger 1959). Solutions to the equation depict the distribution of heat in the subsurface and its variation with time. The partial differential heat equation can be written as:

$$\partial(\rho\,cT)/\partial t = \nabla(\lambda\nabla T) + A - v\nabla T + \alpha\,gT/c \tag{1.5}$$

where the first term on the right hand side of the equation describes the heat conduction (see also Eq. 1.1a), A stands for the depth and material dependent internal heat production (J s^{-1} m^{-3}), the third term describes advective heat transfer (generally mass transfer) and the last term expresses the pressure effect with the density ρ (kg m^{-3}), v velocity (m s^{-1}), g acceleration due to gravity (m s^{-2}) and α (K^{-1}) the volumetric linear coefficient of thermal expansion defined by $\alpha = (1/V)\,\partial V/\partial T$. For most rocks α = 5–25 μK^{-1}.

The analytical solution of Eq. 1.5 for one dimensional heat transport (along depth coordinate z), constant thermal conductivity (λ), constant radiogenic heat production (A), for a homogeneous isotropic volume of rock, no heat transport by mass flux and ignoring the pressure dependence is:

$$T(z) = T_0 + 1/\lambda\, q_0 \Delta z - A/(2\lambda)\Delta z^2 \tag{1.6}$$

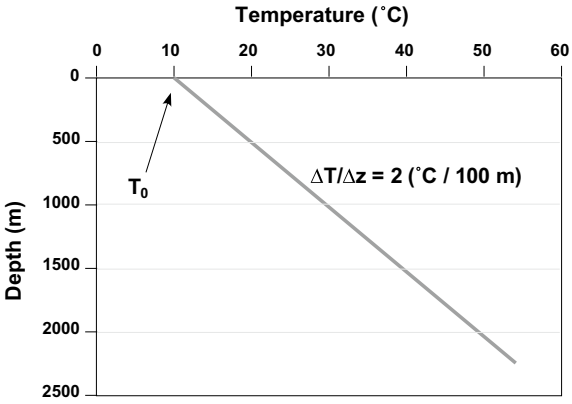

Fig. 1.7 Computed temperature versus depth profile using Eq. 1.6 and the values for the parameters given in the text and on Table 1.1: $T_0 = 283$, $\lambda = 3.1$ J s^{-1} m^{-1} K^{-1} for granite, $q_0 = 65$ mW m^{-2}, $A = 3$ μJ s^{-1} m^{-3} for granite

where T_0 is the temperature at z_0 the top of the considered volume of rock, q_0 the heat flow density at z_0 and Δz the thickness of the considered rock volume. This simplified heat equation (Eq. 1.6) can be used to construct a thermal profile through the crust by adding layer by layer for the case of conductive heat transport and radiogenic heat production in the individual layers (Fig. 1.7).

1.5 Brief Outline of Methods for Measuring Thermal Parameters

Thermal conductivity of rocks can be measured on drillcores in the laboratory or in situ in boreholes directly. There are different methods and types of devices for measuring the thermal conductivity of rocks and soils on the market. All are based on the same principle: the sample is exposed to defined and controlled local heating and temperature sensors measure the temperature response to heating in space and time. The transient line source method is widely used in needle-type measuring instruments. A long and thin heating source is brought in contact with the sample and is heated with constant power, while simultaneously the temperature of the source is registered. The slower the source temperature rises, the higher is the thermal conductivity of the sample material.

Probably the most commonly used method for thermal conductivity measurements in geology is the use of so-called divided bar instruments. The instruments are commercially available also as portable electronic divided bar machines. Portable divided bars apply thermal gradient across a sample along with a substance of known thermal conductivity used as standard. Thermal conductivity of the sample is measured by the device relative to the standard.

Thermal conductivity measuring bars have differential temperature adjustment provisions and provide accurate results with a variance of only 2%. Portable divided bars can be easily calibrated and weigh only 8 kg facilitating easy transport. Divided

bar systems also generate less noise and can be used to measure thermal conductivity of fresh core samples even during remote drilling operations. Additionally, these rock thermal conductivity-measuring bars can provide readings for varying temperatures over a range of 20 °C. Portable thermal conduction measuring devices are very useful in geothermal energy explorations (web page: Hot Dry Rock, Australia).

The heat capacity of rocks is measured with a calorimeter in the laboratory. There are a large variety of calorimeters and the various instruments are used for very different purposes. The parameter C defined in Eq. 1.2a is measured with instruments that add or remove a defined amount of heat to the calorimetric system (sample plus embedding material, usually a liquid) and monitor the temperature response of the process.

The density of rocks in the form of drillcores is measured using Archimedes's principle. This means the mass of an irregularly shaped body like a piece of rock, is first measured by a balance. Then the mass of the body is submerged in a liquid of known density (e.g. water 1000 kg m^{-3} at about 25 ºC and 1 bar) and measured by the balance. The volume of the sample follows from the difference of the two measurements, thus the density $\rho = m/V$ can be calculated from the data. The density of cuttings is measured with a pycnometer, a simple laboratory device for measuring densities of liquids and solids.

1.6 Measuring Subsurface Temperatures

A careful search for existing subsurface temperature data is one of the first and critical steps during the development of a new deep geothermal project. Compiled temperature data from existing old drillholes in the same region greatly facilitate the design of the new installation and dramatically increase the reliability of pre-drilling project forecasts. It is necessary to evaluate the reliability of the data and the exact reading depths.

In Central Europe, for example, the temperature increases with about 3 °C per 100 m depth in the near surface region. This is referred to as the "normal temperature gradient" for the region. This normal regional gradient may deviate in both directions, colder and warmer gradients. Departures from the normal regional gradient may occur in certain depth intervals of a borehole. The deviations from the normal gradient are caused by various local variations of the hydraulic and thermal properties of the geological material underground. The local temperature gradient is constant within a narrow range of near-surface depths. At greater depth the temperature gradient is given by the tangent to the temperature (T) versus depth (z) profile (T-z profile) at each depth (z). The detailed local temperature profile and the associated T-gradient at a site with a given geological structure results from conductive heat flow and from mass flow, which is flow of groundwater or flow of deep fluids. The T-gradient also varies with surface topography. With increasing relief, the T-gradient increases in the valleys and decreases along the ridges.

The SI unit for temperature is Kelvin (K). Derived from Kelvin is the unit Celsius (°C). Other commonly used units are Fahrenheit (°F) and Rankine (°R, also R or Ra). At absolute zero temperature: 0 K = 0 °R. The temperatures can be converted using:

$$T_K = T_C + 273.16 \tag{1.7a}$$

$$T_F = 1.8\,T_C + 32 \tag{1.7b}$$

$$T_R = 1.8\,T_C + 491.67 \tag{1.7c}$$

In deep boreholes the temperature of the liquid phase at the depth z is measured using a temperature sensitive device and the reading is in Ohm (Ω). The resistance is converted to temperature using a Ω−K calibration. The probes need a new calibration after some months in use.

Different types of temperature measurements are distinguished in boreholes:

- Temperature log
- Reservoir temperature or bottom-hole temperature (BHT)
- Temperature measurements during production tests (well tests).

Temperature logs are T data from continuous T measurements along the borehole profile. It is important to pay attention to the time of logging: During production, shortly after production or after a long downtime. The most useful data are produced after long downtime (Fig. 1.8). T-logs influenced by the production operation often provide meaningful T data only at the sites (depth) of water inflow points. T-logs can provide evidence of water inflow and outflow points (fluid sinks) (Fig. 6.19), leaks in the casing or vertical fluid flow (Fig. 13.5). Temperature data collected during production tests provide access to the vertical distribution of the hydraulic conductivity. (Fig. 14.10). Detailed treatment of hydraulic evaluation procedures can be found in Sects. 14.2 and 14.4.

BHT measurements are performed routinely immediately after completion of the industrial drill hole. Thus the data are commonly thermally disrupted by e.g. friction and circulation of drilling fluid. These BHT data can be corrected for these effects and reduced to the pristine situation, particularly because the influences of drilling fluid circulation on the temperature field are lowest at bottom hole. Commonly there are several BHT data available for most drill holes, often also for different depths that have been collected during an incremental drilling progress.

Different temperature extrapolation procedures are used depending on the downtime after completion of the drillhole, the duration of the flushing period, and the number of available temperature data:

- The “explosion cylinder source” (Leblanc et al. 1982)
- The “continuous line source” (Horner 1951)
- The “explosion line source” (Lachenbruch & Brewer 1959)
- The “cylinder source with statistical parameters” (Middleton 1982).

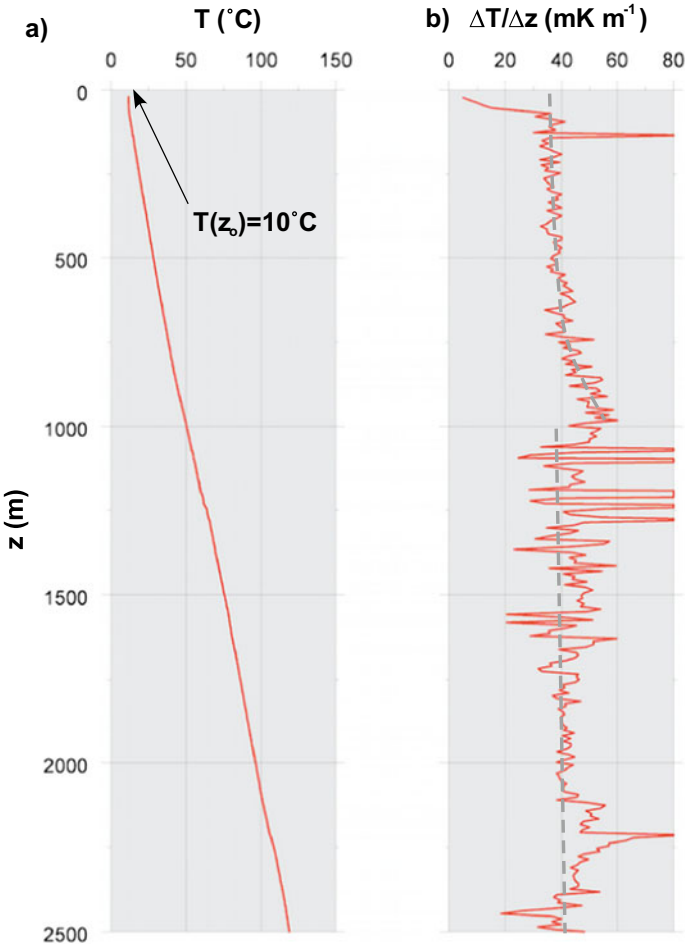

Fig. 1.8 Example of a T-log after a long downtime in the well Bühl in the upper Rhine rift valley (Germany) (Schellschmidt & Stober 2008): **a** T-profile; **b** T-gradient ($\Delta T/\Delta z$). Note that the striking gradient variations relate to small Δz between readings and thus are mostly caused by the technique and only to a minor extent related to the geology along the profile

Extrapolation of a single BHT measurement to the pristine pre-drilling temperature at bottom hole requires a derivation of statistical parameters from additional temperature data in the borehole.

The thermal conductivity of the formation can be derived from the temperature response of the probe installed during a production test. For this purpose the temperature is continuously recorded by the probe at a fixed position within the formation of interest. The procedure is analogous to the technique described in Fig. 6.8. The pristine temperature at the position of the probe can be deduced from the T data during the adjustment period using a so-called Horner Diagram (Horner 1951).

Temperature maps at a depth of interest can be constructed from interpolated temperature data in both horizontal and vertical direction. Different techniques exist for this purpose including the "gridding algorithm" (Smith & Wessel 1990).

For the computation of a three dimensional temperature model along the drill hole the temperature of the topsoil layer must be known. It defines the upper boundary limit of the model. The temperature (T_0) can be derived from long time annual averages of the local air temperature using data compiled by the local weather services or from the World Meteorological Organization (NCDC 2002). The average annual near ground surface temperature of the air corresponds is close to the soil or rock temperature at 13 m below the surface (in central Europe). At this depth the ground temperature does not vary with the season. Data interpolation for the model can be carried out utilizing a 3D universal Kriging method.

References

Ahrens, T. J., 1995. Global Earth Physics: a Handbook of Physical Constants. Am. Geophys. Union, 376 pp.

Armstead, H. C. H., 1983. Geothermal Energy. E. & F. N. Spon, London, 404 pp.

Carslaw, H. S. & Jaeger, J. C., 1959. Conduction of Heat in Solids. Oxford at the Clarendon Press, Oxford, 342 pp.

Clauser, C., 2009. Heat Transport Processes in the Earth's Crust. Surveys in Geophysics, **30**, 163–191.

Horner, D. R., 1951. Pressure Build-up in Wells. In: Bull, E. J. (ed.): Proc. 3rd World Petrol. Congr., pp. 503–521, Leiden, Netherlands.

Kappelmeyer, O. & Haenel, R., 1974. Geothermics with special reference to application, pp. 238, E. Schweizerbart Science Publishers, Stuttgart.

Lachenbruch, A. H. & Brewer, M. C., 1959. Dissipation of the temperature effect of drilling a well in Arctic Alaska. - Geological Survey Bulletin, 1083-C: 73–109; Washington.

Landolt-Börnstein, 1992. Numerical Data and Funktional Relationships in Science and Technology. In: Physical Properties of Rocks, Springer, Berlin-Heidelberg-New York.

Leblanc, Y., Lam, H.-L., Pascoe, L. J., & Johnes, F. W., 1982. A comparison of two methods of estimating static formation temperature from well logs. Geophys. Prosp., 30, 348-357.

Mareschal, J.-C. & Jaupart, C., 2013. Radiogenic heat production, thermal regime and evolution of the continental crust. Tectonophysics, 609, 524-534.

Middleton, M. F., 1982. Bottom-hole temperature stabilization with continued circulation of drilling mud. Geophysics, 47, 1716-1723.

NCDC, 2002. WMO Global Standard Normals (DSI-9641A), Asheville (USA) (Nat. Climatic Data Center).

Pollack, H. N., Hurter, S. J. & Johnson, J. R., 1993. Heat Flow from the Earth's Interior - Analysis of the Global Data Set. Rev. Geophys, 31, 267-280.

REN21., 2017. Renewables 2017 Global Status Report.- Paris Ren21 Secretariat, https://www.ren21.net.

Rybach, L., 1976. Radioactive heat production in rocks and its relation to other petrophysical parameters. Pageoph (114), 309–317.

Schädel, K. & Stober, I., 1984. The thermal anomaly of Urach seen from a geological perspective (in German). Geol. Abh. Geol. Landesamt Baden-Württemberg, 26, 19-25.

Schellschmidt, R. & Stober, I., 2008. Untergrundtemperaturen in Baden-Württemberg.- LGRB-Fachbericht, 2, 28 S., Regierungspräsidium Freiburg.

Schön, J., 2004. Physical properties of rocks, pp. 600, Elsevier.
Smith, W. H. F. & Wessel, P., 1990. Gridding with continuous curvature splines in tension. Geophysics, 55: 293-305.
U.S. Department of Energy., 2016. 2016 Renewable Energy Data Book, Energy Efficiency & Renewable Energy of the National Renewable Energy Laboratory (NREL) (https://www.nrel.gov).
VDI, 2001. Use of suburface thermal resources (in German). Union of German Engineers (VDI), Richtlinienreihe, 4640.

Chapter 2
History of Geothermal Energy Use

Huaqin Hot Springs near Xi'an, China

I. Stober and K. Bucher, *Geothermal Energy*,
https://doi.org/10.1007/978-3-030-71685-1_2